Model reduction for simulating the dynamic behavior of parabolic troughs and a thermocline energy storage in a micro-solar power unit

Rémi Dickes[a], Adriano Desideri[a], Vincent Lemort[a] and Sylvain Quoilin[a]

[a] Energy Systems Research Unit
Aerospace and Mechanical Engineering Department,
Faculty of Applied Sciences
University of Liège
Belgium
Contact: rdickes@ulg.ac.be

Abstract:

Micro-scale concentrated solar power plants are characterized by strong transients and mostly operate in off-design working conditions. Both the sizing and the control of these systems are key challenges whose optimization requires powerful dynamic modeling tools. In this context, a system featuring a solar field of parabolic troughs, a thermocline thermal energy storage and a 5kW$_e$ organic Rankine cycle (ORC) power unit is modeled in the Modelica language. Model reduction methods applied to the solar field and the thermal storage are investigated and analyzed to improve the computational efficiency of the problem. Each model is described and integrated in the open-source ThermoCycle library. Results of simulation under identical operating conditions are compared and the benefits and limitations of model reduction are assessed.

Keywords:

Dynamic modeling reduction, Concentrated solar power, Thermocline storage, Parabolic trough

1. Introduction

Global warming and energy security issues due to the dependency on fossil fuels are nowadays almost universally recognized. For these reasons, concentrated solar power (CSP) systems, together with other renewable energy technologies, are increasingly developed [1, 2]. Besides already-mature large-scale applications, CSP principle can be used in micro-scale facilities (called µCSP) for generating electricity and useful heat in remote off-grid areas, e.g. in developing countries [3]. Because of the intermittent nature of both the solar irradiance and the local energy demand, such µCSP systems are submitted to strong transients and almost never operate in nominal working conditions. Both the sizing and the control of these systems are key challenges which require powerful dynamic modeling tools. Robustness, accuracy and low simulation time are fundamental characteristics required for the direct applications of dynamic modelling tools in optimisation problems [4].

In this context, model reduction for simulating a micro-scale solar power plant is investigated. The system studied in this contribution is depicted in Fig. 1. It features a solar field of parabolic troughs (130 m^2), a thermocline storage tank (8m^3) and a 5 kW$_e$ non-recuperative Rankine cycle using R245fa as working fluid. The heat transfer fluid is Therminol 66 and the mass flow rates through the solar field, the thermal energy storage and the evaporator of the organic Rankine cycle (ORC) are controlled by two external pumps. The working principle of the system can be summarized as follows: the heat transfer fluid (HTF) is pumped to the solar collectors and it gets heated up. It then flows through the evaporator where the thermal power is transferred to the ORC unit. From the evaporator outlet, the HTF is sent back to the solar field to be heated up again. At times of high solar irradiation, the thermal energy surplus is stored into the thermal energy storage (TES). From there, energy is extracted to compensate for low radiation period e.g. unfavourable meteorological conditions.

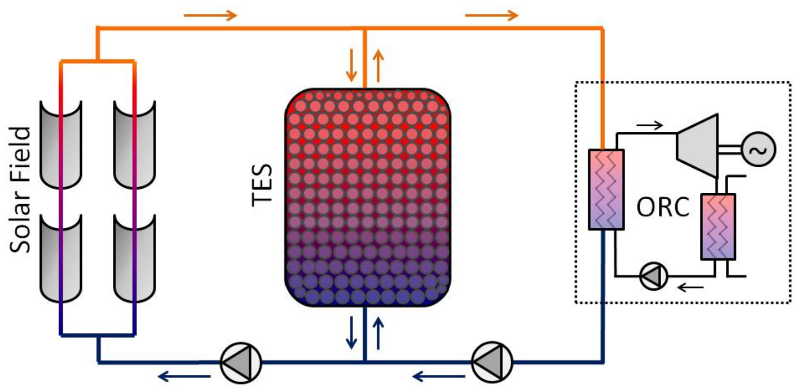

Fig. 1: Schematic layout of the µCSP systems studied in this work.

The goal of this contribution is to assess the benefits and limitations of model reduction for simulating this system. For the sake of conciseness, neither the control strategy nor technical data of the system are described in this paper. A more detailed description of the system is available in [5].

2. Models description

This section is dedicated to the description of the models developed to simulate the aforementioned solar system. Both the solar field and the thermocline storage are investigated in detail. Model reduction of the organic Rankine cycle is under investigation and will be the object of a future work. The models are developed in the Modelica language and they are included in the open-source ThermoCycle library [6] dedicated to the modeling of thermal systems and under development at the University of Liège since 2009.

2.1 – Solar thermal collectors

Parabolic trough collectors (PTCs) are linear parabolic mirrors focusing sunlight on a heat collector element (HCE) placed along the focal line. In order to evaluate the temperature profile of the fluid circulating along the collectors, the most common approach is to discretize the tube receiver along its axial axis in a number of cells of constant volume , N_{SF}, as shown in Fig. 2. The temperature profile is calculated by evaluating the energy balance in each cell, assuming an incompressible flow, i.e.

$$T_{i+1} = T_i + \frac{\dot{Q}_{abs,i}}{\dot{m}\, cp_{HTF,i}} \quad , \quad \forall i \in [1, N_{SF} - 1] \tag{1}$$

where T_i is the fluid temperature of the ith node, $\dot{Q}_{abs,i}$ is the net heat power absorbed by the fluid in the ith cell, $\dot{m}$ is the HTF mass flow rate and cp_{HTF} is the fluid specific heat capacity.

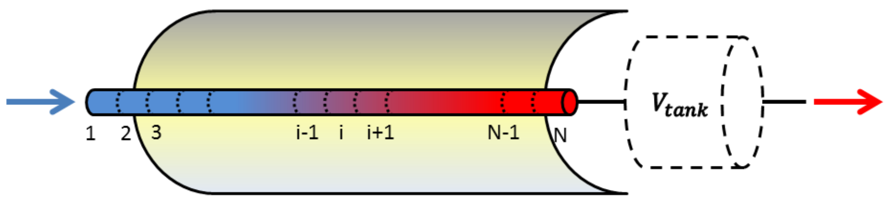

Fig. 2: One-dimensional discretization of the PTC with the fictive tank connected to the SF outlet.

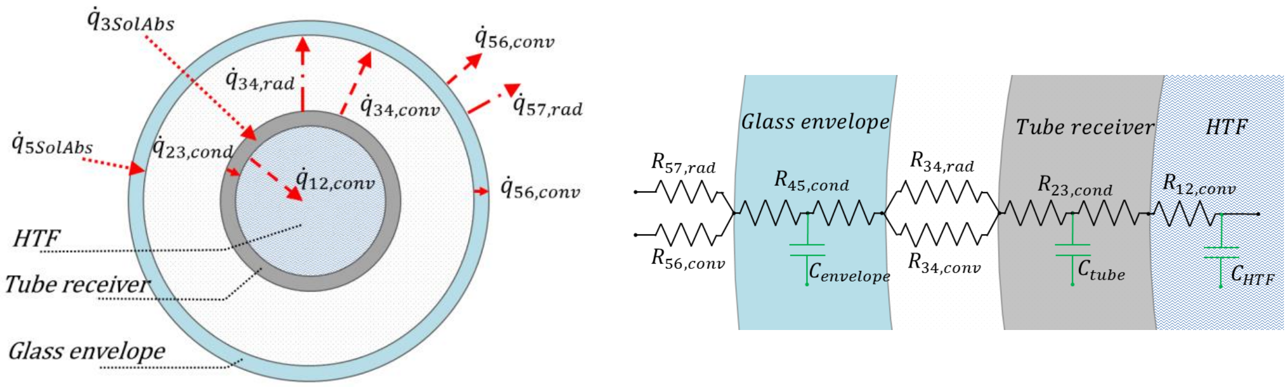

Fig. 3: Complete radial heat balance inside a heat collection element, adapted from [7] (left). Illustration of the equivalent resistance scheme including the thermal capacitances (right).

2.1.1. Detailed model

To calculate the net heat power in (1), a physically-based approach consists in solving the radial heat balance between the heat transfer fluid, the tube receiver, the glass envelope and the surrounding environment, as depicted in Fig. 3. This can be achieved using Forristal's deterministic model [7], widely used in the literature and accounting for each conductive, radiative and convective heat exchanges. In this work, this model is implemented in the Modelica language [8]. However, Forristal's equations correspond to a steady-state equilibrium along parabolic trough collectors and do not account of the dynamic response in case of transient working conditions. The thermal capacitances of the glass envelope, the tube receiver and the fluid are therefore included to complement Forristal's initial model, as illustrated in Fig. 3. The number of cells N_{SF} used to discretize the HCE is a key parameter and influences the simulation results. It must be high enough to limit numerical diffusion [9]. However, the higher the number of cells, the higher the number of equations and the lower the simulation speed, as discussed in section 3.2.

2.1.2. Reduced model

An alternative method to reduce the simulation complexity is to calculate the steady-state temperature profile along the solar collectors without solving the radial heat balance in each cell. The idea is that it is possible to derive the absorbed heat power in (1) by means of a calibrated correlation which calculates the effective heat losses of the HCE in function of the working conditions. Among the different correlations existing in the literature, the polynomial relation proposed by the authors [10] is chosen in this work i.e.

$$HL = a_0 + a_1\left(T_{htf} - T_{amb}\right) + a_2\left(T_{htf} - T_{amb}\right)^2 + DNI\cos(\theta)\left(a_3 {T_{htf}}^2 + a_4\sqrt{v_{wind}}\right) + a_5 {T_{htf}}^3 + v_{wind}\left(a_6 + a_7\left(T_{htf} - T_{amb}\right)\right) + \sqrt{v_{wind}}\left(a_8 + a_9\left(T_{htf} - T_{amb}\right)\right) \quad (2)$$

where HL (W/m) is the effective linear heat losses of the HCE, $T_{htf}(°C)$ is the fluid temperature, $T_{amb}(°C)$ is the ambient temperature, $DNI(W/m^2)$ is the direct solar irradiance, θ (rad) is the incidence angle and v_{wind} (m/s) is the surrounding wind speed. Using (2), the heat power absorbed by the fluid in each cell can be easily computed as described in detail in [10]. Finally, to account for the overall thermal inertia of the solar field, a hypothetical fluid reservoir is connected to the PTCs outlet, as shown in Fig. 2. This reservoir acts as a dynamic damper and smooth out the temperature changes simulated by steady-state model at the solar field outlet.

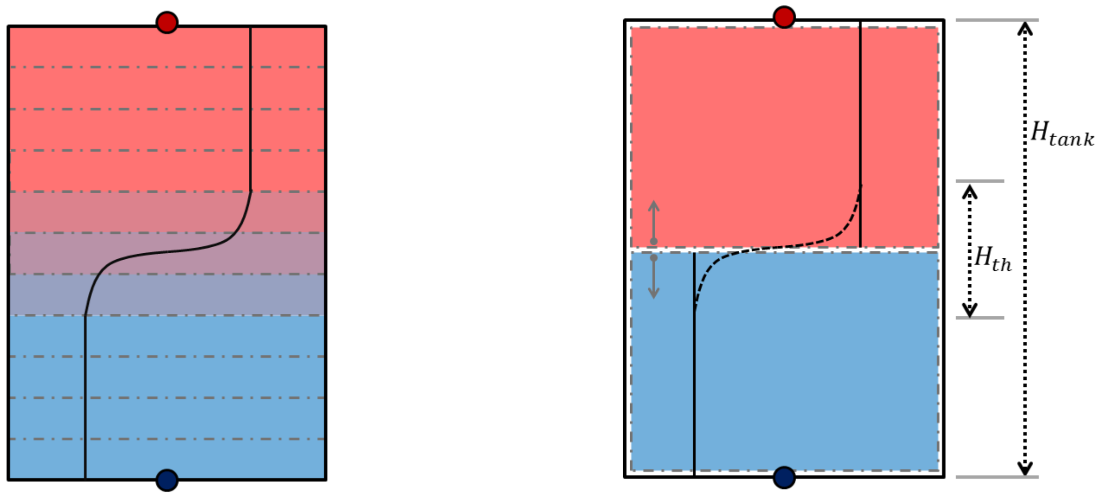

(a) One-dimensional finite-volume method *(b) Two-zone moving-boundary method*

Fig. 4: Modeling methods of the thermocline storage.

2.2 – Thermocline storage

Up to now, double-tank storage configuration is the preferred thermal energy storage technology in commercial CSP plants [11]. However, important cost reductions could be achieved by using single-tank technologies such as thermocline storage units [12]. In such a system, both hot and cold fluids are stored in a same tank by taking advantage of the thermal stratification due to the density difference linked to the fluid temperature gradient. Despite of the great potential of cost reduction, thermocline TES still present many challenges regarding their integration and their control in CSP power plants.

2.2.1. Detailed model

In a physically-based approach, a thermocline system can be modeled with a one-dimensional finite-volume method as described in [5, 13]. The storage tank is assumed cylindrical and discretized along its vertical axis in a finite number of isothermal cells, N_{TES}, as depicted in Fig. 4a. The model can either simulate liquid-only or packed-bed storage systems. It accounts for the conductive heat transfer in the surrounding metal casing, the fluid and the filler material. Temperatures of the fluid and the filler material in the same cell are assumed equal in the case of a packed-bed TES. It also accounts for the heat losses to the environment and flow reversal in case of discharging and charging modes. The dynamic behavior and the temperature profile inside the tank are calculated by evaluating the mass and energy balances in each cell for each time step.

The model has been validated both in charging and discharging processes with experimental data found in the scientific literature [14, 15]. Fig. 5 shows the experimental validation in discharge and demonstrates the strong link between N_{TES} and the temperature profile predicted inside the tank. It can be noted that there is a significant influence of the number of cells on the predicted temperature profile. This is due to the "numerical diffusion" effect, i.e. the smoothing effect due to the successive ideal-mixing of the fluid in each cell. The number of cells must therefore be high-enough to limit this effect, which also has a negative effect on the computational efficiency. According to Fig. 5, the number of nodes required to achieve an acceptable limited numerical diffusion is about 100, which leads to a high simulation time, as demonstrated in section 3.2.

It should also be noted that this model does not account for the effect of a temperature inversion inside the thermocline storage. A temperature inversion occurs when the HTF enters at the top (resp. bottom) of the TES with a colder (resp. warmer) temperature than the temperature in the

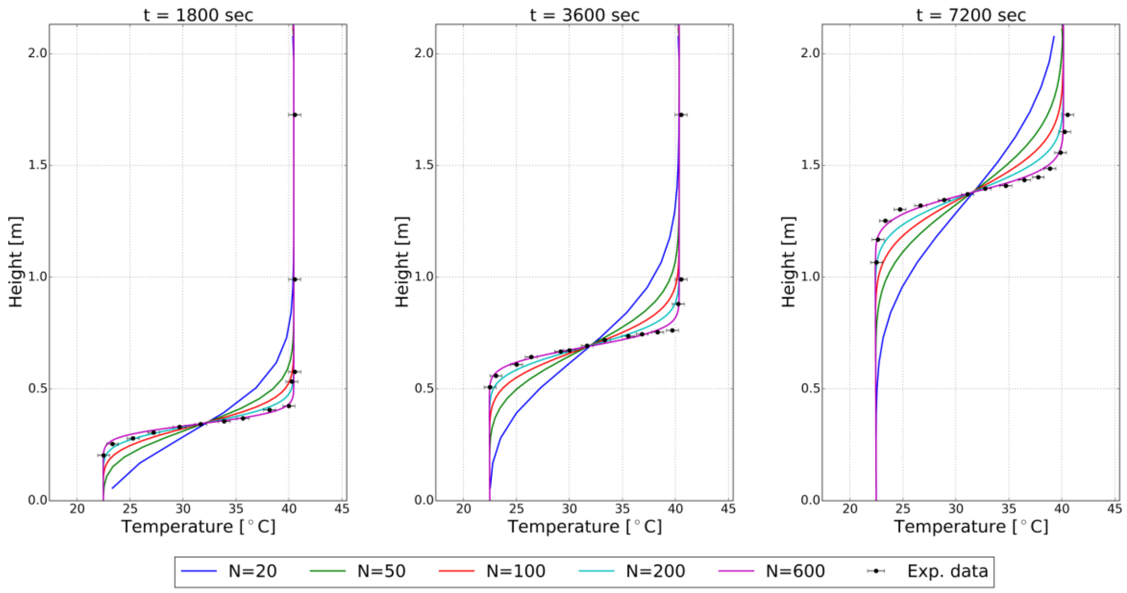

Fig. 5: Temperature profiles along the tank simulated by the complex model (with various numbers of cells) at three different times and compared to experimental measurements [14].

upper (resp. lower) zone of the tank, as illustrated in Fig. 6. In such scenario, the density gradient is inverted and buoyancy forces induce a mixing of the fluid. Modeling this mixing process is a real challenge and adds further complexity to the model [16]. However, since thermocline TES systems take advantage of the thermal stratification inside the tank, the TES integration in the power plant and the control strategy of the charging/discharging processes must be defined to avoid any temperature inversion. Therefore, the ability of modeling such phenomena is not relevant.

2.2.2. Reduced model

Another approach to simulate thermocline storage is to use a two-zone moving-boundary model. Following this method depicted in Fig. 4b, the thermal energy storage is divided in two isothermal zones, a *hot zone* and a *cold zone*, of variable volumes. Volume and enthalpy variations in the two zones are calculated independently by evaluating both the mass and the energy balances. In the case of a complete charge or discharge of the TES, the model switches to a single-cell model.

Although the simulation speed is dramatically increased (only two cells are required to simulate the TES), this new approach assumes a perfect thermocline region of zero thickness, which is not the case in reality. Besides of the temperature discontinuity observed at the TES port in case of complete dis/charge of the tank (which leads to modeling robustness issues), the assumption of a perfect stratification overestimates the TES performance. To overcome this problem, a hypothetical transition profile of the temperature centered on the ideal separation line is implemented, as illustrated in Fig. 4b. The normalized thickness L_{th} of the hypothetical transition profile is a parameter of the model and is defined i.e.

$$L_{th} = \frac{H_{th}}{H_{tank}}$$

where $H_{th}(m)$ is the thickness of the thermocline and $H_{tank}(m)$ is the height of the tank, as depicted in Fig. 4b.

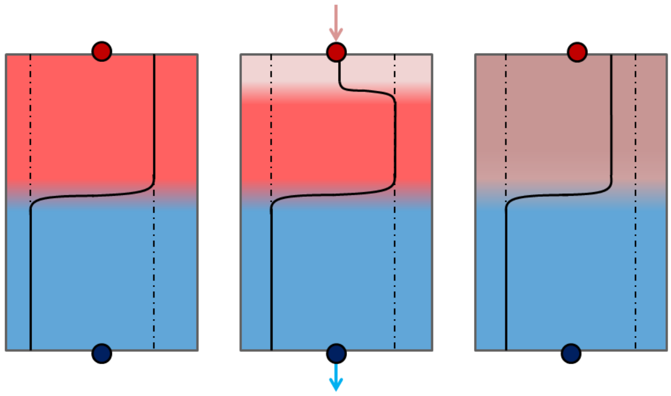

Fig. 6: Thermocline degradation due to a temperature inversion inside the tank [4]

3. Results analysis and comparison

The benefits and limitations of modeling reduction are evaluated in this last section. Both the thermocline system and the solar field are simulated using the above models with identical boundary conditions. The performance of these models is analysed in terms of simulation speed and deviations with respect to the results of the physically-based models.

3.1 – Solar thermal collectors

In order to assess the two approaches described in section 2.1, the temperature evolutions at the solar collector outlet is simulated during a whole day using four different models. The four models, referred to as SF_A, SF_B, $SF_C$and SF_D, are defined as follows:

- SF_A : physically-based model implementing Forristal's equations and accounting for the system thermal inertia in each cell;
- SF_B: steady-state model implementing only the semi-empirical correlation (2), without any fictive tank connected to the outlet;
- SF_C : identical to SF_B but with the inclusion of a fictive tank at the outlet having a volume equal to the volume of HTF in the solar field ($V_{tank,SF_C} = V_{HTF}$),
- SF_D : identical to SF_C but with a volume optimized to reproduce the response of SF_A.

Simulation results for the complete day are depicted in Fig. 7, together with two enlarged views at the beginning and the end of the day for additional clarity. Identical operating conditions and input parameters are used for the four simulations. The solar irradiance DNI corresponds to Almeria in 1996, July 10th, and was selected because of the availability of high temporal resolution solar irradiation data. The inlet temperature of the solar field T_{su} and the HTF mass flow rate $\dot{m}$ verify the control strategy described in [4]. Several conclusions can be drawn from the simulation results.

During transient periods, there is an important deviation between the steady-state SF_B model and the reference profile SF_A. For example, at the beginning of the day (t ≈ 2h), the sun starts shining over the solar field and the HTF is circulated through the solar field where it is heated up to the nominal temperature. During this period, the steady-state response gets ahead the dynamic profile by around 7 minutes, leading to an instantaneous temperature error at the solar field outlet up to 60 K. Such a mismatch leads to the conclusion that the dynamics characterizing the solar field cannot be neglected.

Models SF_C and SF_D present a response closer to the reference one. The fictive tank added at the outlet acts as a damper of the steady-state response and allows accounting for the solar field thermal inertia. Substantial deviation compared to the reference model is still present. The simplified models do not consider the time delay due to temperature propagation in the parabolic trough collectors. A transfer function accounting for such delay in the inlet working conditions could be a good alternative for modeling improvement and it will be investigated in a future work by the authors. Nevertheless, the errors committed by the model SF_D remain local and are assumed negligible over long-term simulations.

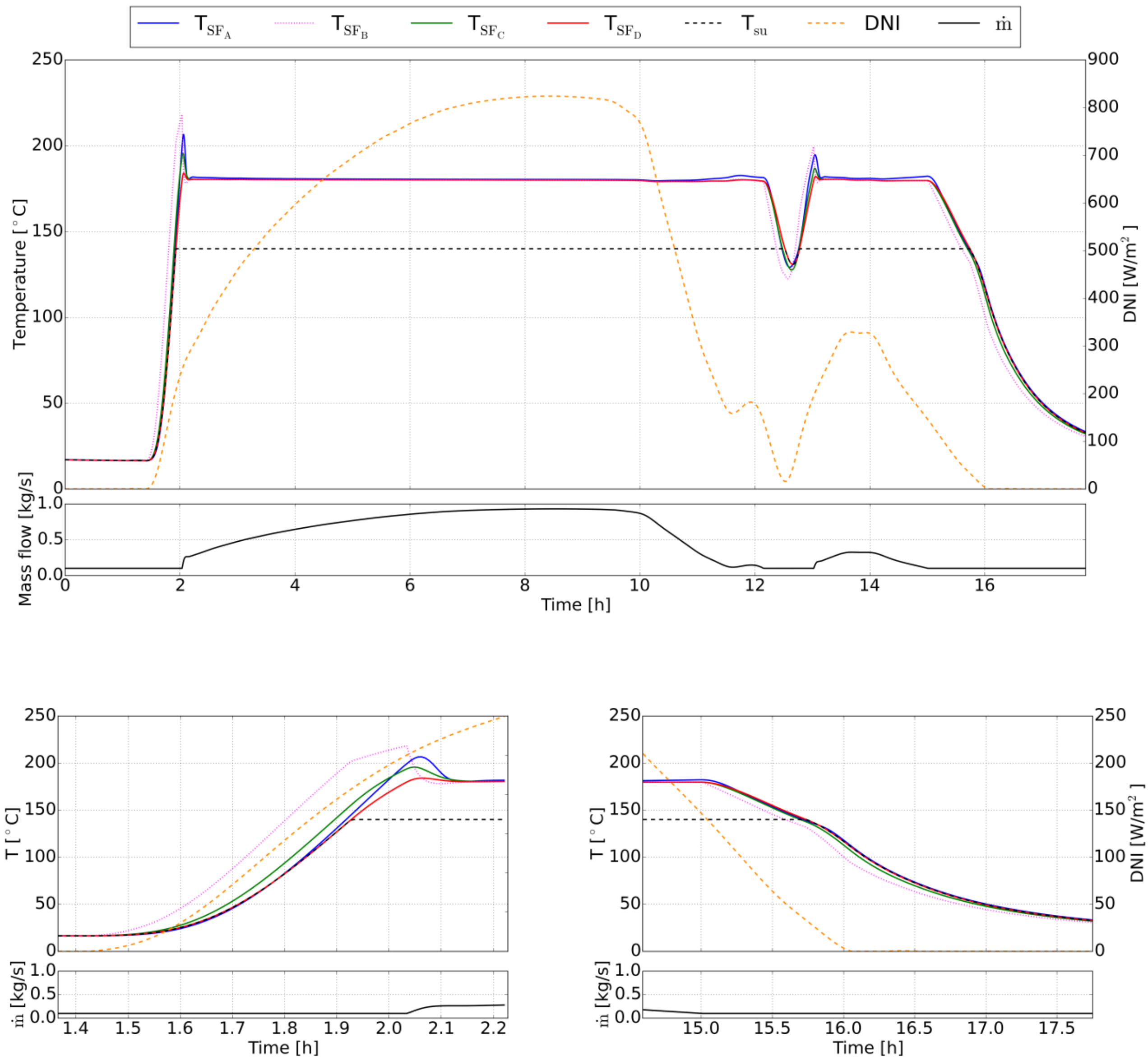

Fig. 7: Temperature profiles with respect to time at the solar field outlet predicted by the four different models: model SF_A (in blue), model SF_b (in dotted purple), model SF_C (in green) and model SF_D (in red).

Table 1. Integration times and number of variables required for modeling three reference days

Model	Number of cells (-)	Integration time (sec)	Number of variables (-)
SF_A	10	40.1	780
SF_A	25	75.2	1700
SF_B	10	15.1	95
SF_B	25	17.9	155
$SF_{C,D}$	10	18	108
$SF_{C,D}$	25	22.1	168

The computation time of the models is assessed by performing a simulation over three reference days imposing the number of cells to 10 and 25 for each method. The results are summarized in Table 1: the simulation speed is dramatically decreased when using the simplified methods. Indeed, the complex approach requires solving the complete radial heat balance in each cell to derive the net heat power absorbed by the fluid. Furthermore, the thermal inertia of the glass envelope, the tube receiver and the fluid are taken into account in each cell, leading to a high number of differential equations to be evaluated at each time step. On the other hand, the reduced model uses a single semi-empirical correlation to derive the effective heat power absorbed by the HTF and a unique fictitious fluid volume simulates the overall system dynamics.

3.2 – Thermocline storage

In order to assess the benefits and limitations of the two approaches described in section 2.2, the temperature profiles of the thermocline storage predicted using three different models are compared. The case of a complete charging process is depicted in Fig. 8, but similar results can be observed with other operating scenarios. The three models are defined as follows:

- TES_A: physically-based model implementing the one-dimensional finite-volume approach with 200 cells, as described in section 2.2.1;
- TES_B: simplified model based on the basic two-zone moving-boundary method given in section 2.2.2;
- TES_C: similar to TES_B but with a transition profile integrated between the two zones in order to simulate the thermocline stratification.

Several observations can be made from the simulation results given in Fig. 8. First, the simplified two-zone moving-boundary method simulates correctly the progression of the thermocline along the TES vertical axis: the effective thermocline zone simulated by the discretized method

Table 2. Integration times and number of variables for modeling a complete charge of the tank

Model	Number of cells (-)	Integration time (sec)	Number of variables(-)
TES_A	20	26	600
TES_A	50	59	1470
TES_A	100	160	2920
TES_A	200	525	5820
TES_B	2	4,5	75
TES_C	2	5	80

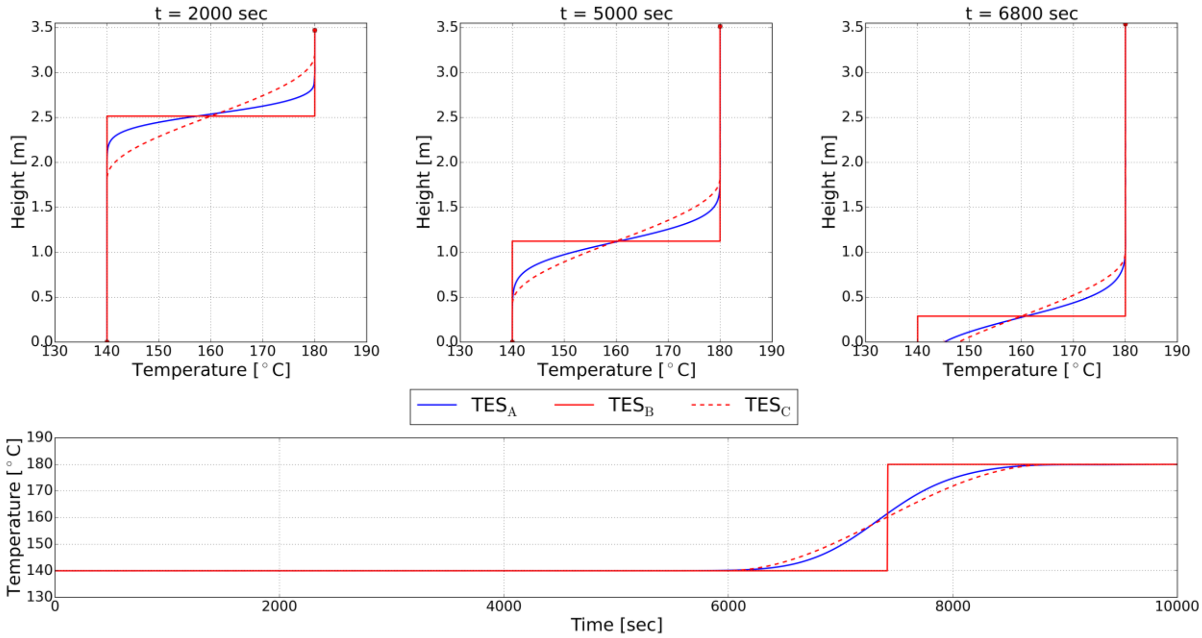

Fig. 8: For the three different TES model: temperature profiles inside the tank during the charging process (up). Temperature at the TES bottom port as a function of time (bottom).

remains centered on the ideal separation line between the hot and cold zone predicted by model TES_B. Secondly, the thermocline thickness does not remain constant during the charging process. At the beginning of the charge, the thermocline is almost ideal with a very low thickness. Then, the thermocline expands gradually in the tank due to the thermal diffusion between the hot and the cold zones. However, the transition profile implemented in model TES_C assumes a constant thermocline thickness, whatever the operating conditions. From the results of several additional simulations of TES_A, it has been observed that the thermocline relative thickness L_{th} remains close to a constant value ($L_{th} \approx 0.4$) when reaching the extraction port, either in charging and discharging processes. In Fig. 8, the temperature profiles observed at the bottom port show a minor deviation between the results of the models TES_A and TES_C. Finally, the simulation speed of the three TES models is assessed by comparing the integration time for a complete charging process. The results, shown in Table 2, underline the capability of the moving-boundary method to decrease the simulation time. Another important characteristic of the moving-boundary method over the complex model is its ability to simulate conservative performance of the storage by imposing an overestimated constant thickness of the thermocline.

4. Conclusion

Micro-scale concentrated solar power plants are characterized by strong transients and mostly operate in off-design operating conditions. Both the sizing and the control of these systems are challenges which require the optimization of dynamic modelling tools. In this context, a system featuring a solar field of parabolic troughs, a thermocline unit and a 5kWe power unit is modeled in the Modelica language. Model reduction methods for the solar field and the thermal storage unit are proposed to reduce the model complexity, increase its robustness, and finally decrease the simulation time. To this end, complex and simplified models are developed and the results of simulation in identical operating conditions are compared. The different models are implemented in the open-source ThermoCycle library and are readily accessible to the interested reader.

The simplified model of the solar field proposed in this work is based on a semi-empirical correlation to compute the steady-state temperature profile along the parabolic troughs. The overall dynamics of the system is simulated by a fictitious HTF fluid volume connected in series with the

solar field outlet. A good agreement is achieved in most transient and steady-state operating conditions. Significant deviations are observed for fast transient conditions (i.e. with time constants lower than the residence time of the fluid within the collectors). This is due to the use of a single thermal inertia which does not properly model the progression of the temperature gradients within the collector tubes. However, these fast effects are localized and remain negligible in long-term simulations. A continuous time-delay transfer function could be a good solution to this issue and will be the object of future investigations. Regarding thermal storage, this work proposes a reduced model based on a two-zone moving-boundary method integrated with a transition temperature profile. This approach reduces the simulation time by 99.1% and reproduces fairly well the predictions of the detailed model. A possible modeling improvement could consist in the dynamic update of the thermocline thickness in function of the operating conditions.
In future works, these reduced models will be further improved and validated over a wider range of operating conditions. The results presented in this paper however tend to demonstrated that it is possible to define reduced models with a good accuracy and with significant improvements in terms of complexity, robustness and computational efficiency.

Nomenclature

Acronyms

CSP	Concentrated Solar Power
DNI	Direct Normal Irradiance
HCE	Heat Collection Element
HTF	Heat Transfer Fluid
ORC	Organic Rankine Cycle
SF	Solar Field
PTC	Parabolic Trough Collectors
TES	Thermal Energy Storage

Subscripts

abs	absorbed
amb	ambient
cond	conduction
conv	convection
rad	radiative
th	thermocline
wind	surrounding wind

Symbols

C	Thermal capacitance, J/K
cp	Specific heat capacity, J/kg.K
H	Height, m
HL	Linear heat losses, W/m
L	Normalized thickness, -
$\dot{m}$	Mass flow rate, kg/s
N	Number of cells

$\dot{Q}$	Heat power, W
$\dot{q}$	Heat flux, W/m²
R	Thermal resistance, K.m²/W
T	Temperature, °C
v	Velocity, m/s
V	Volume, m³
θ	Incidence angle, rad

References

[1] Price, H., Hassani, V., 2002. Modular Trough Power Plant Cycle and System Analysis. Technical Report NREL/TP-550-31240, National Renewable Energy Laboratory.

[2] International Energy Agency. 2014. Article: "How solar energy could be the largest source of electricity by mid-century".Available at: < http://www.iea.org>.

[3] Dickes, R., 2013. Design and fabrication of a variable wall thickness two-stage scroll expander to integrated in a micro-solar power plant. Master Thesis, University of Liège.

[4] Casella, F.; Mathijssen, T.; Colonna, P., van Buijtenen, J., 2013. Dynamic modeling of Organic Rankine Cycle power systems. Journal of Engineering for Gas Turbine and Power. Vol 135

[5] Dickes, R., Desideri, A., Bell, I., Quoilin, S., Lemort, V., 2014. Dynamic modeling and control strategy analysis of a micro-scale CSP plant coupled with a thermocline system for power generation. Conference proceedings. EuroSun 2014, France, September.

[6] Quoilin, S., Desideri, A., Wronski, J., Bell, I., Lemort, V., 2014. Thermocycle: a Modelica library for the simulation of thermodynamic systems. Proceedings of the 10th international Modelica conference

[7] Forristal, R., 2003. Heat transfer analysis and modeling of a parabolic trough solar receiver implemented in EES. Technical report NREL/TP-550-34169. National Renewable Energy Laboratory

[8] Casati, E., Galli, A., Colonna, P., 2012. Preliminary assessment of a novel small CSP plant based on linear collectors, ORC and direct thermal storage. Conference proceeding of SolarPACES 2012.

[9] Lai C, Bodvarsson G., 1986. A second-order Upwind Differencing Method for Convection-Diffusions equations. Earth Sci Div Annu Rep. 93–7.

[10] Dickes, R., Lemort, V., Quoilin, S., 2015. Semi-empirical correlation to model heat losses along solar parabolic trough collectors. Proceedings of the 28th ECOS conference. Under review.

[11] Kuravi, S., Trahan, J., Goswamind, Y., Rahmanand, M., Stefanako, E., 2013. Thermal energy storage technologies and systems for concentrating solar power plants Progress in Energy and Combustion Science. Vol 39, 285-319

[12] Bayón, R., Rojas, E., 2014. Analytical function describing the behavior of a thermocline storage tank: a requirement for annual simulations of solar thermal power plants. International Journal of Heat and Mass transfer. 68, 641-648.

[13] Galli, A., 2001. Assessment of direct working fluid storage concepts for ORC power systems. PhD Thesis, Politecnico di Milano.

[14] Zurigat, Y., Lich, P., Ghajar, A., 1991. Influence of inlet geometry on mixing in thermocline thermal energy storage. International Journal of Heat and Mass Transfer. 34, 115-125.

[15] Pacheco, J., Showlater, S., Kolb, W., 2002. Development of a molten-salt thermocline thermal storage system for parabolic trough plants. Journal of Solar Energy Engineering. 124, 153-159.

[16] Powell, K. M., Edgar, T. F., 2013. An adaptive-grid model for dynamic simulation of thermocline thermal energy storage system. Energy Conversion and Management, 76, 865-873